Ligand-Induced Conformational and Structural Dynamics Changes in Escherichia coli Cyclic AMP Receptor Protein †

ARTICLE *in* BIOCHEMISTRY · JUNE 2002

Impact Factor: 3.02 · DOI: 10.1021/bi020036z · Source: PubMed

5 AUTHORS, INCLUDING:

Aichun Dong
University of Northern Colorado
54 PUBLICATIONS **4,374** CITATIONS
SEE PROFILE

Jedrzej Malecki
University of Oslo
19 PUBLICATIONS **449** CITATIONS
SEE PROFILE

James Ching Lee
University of Texas Medical Branch at Galves…
140 PUBLICATIONS **5,725** CITATIONS
SEE PROFILE

Ligand-Induced Conformational and Structural Dynamics Changes in *Escherichia coli* Cyclic AMP Receptor Protein†

Aichun Dong,‡,§ Jedrzej M. Malecki,‡ Lucy Lee,‡ John F. Carpenter,|| and J. Ching Lee*,‡

Department of Human Biological Chemistry and Genetics, University of Texas Medical Branch, Galveston, Texas 77555-1055, and Department of Pharmaceutical Sciences, University of Colorado Health Sciences Center, Denver, Colorado 80262

Received January 15, 2002; Revised Manuscript Received March 7, 2002

ABSTRACT: Cyclic AMP receptor protein (CRP) regulates the expression of a large number of genes in *E. coli*. It is activated by cAMP binding, which leads to some yet undefined conformational changes. These changes do not involve significant redistribution of secondary structures. A potential mechanism of activation is a ligand-induced change in structural dynamics. Hence, the cAMP-mediated conformational and structural dynamics changes in the wild-type CRP were investigated using hydrogen−deuterium exchange and Fourier transform infrared spectroscopy. Upon cAMP binding, the two functional domains within the wild-type CRP undergo conformational and structural dynamics changes in two opposite directions. While the smaller DNA-binding domain becomes more flexible, the larger cAMP-binding domain shifts to a less dynamic conformation, evidenced by a faster and a slower amide H−D exchange, respectively. To a lesser extent, binding of cGMP, a nonfunctional analogue of cAMP, also stabilizes the cAMP-binding domain, but it fails to mimic the relaxation effect of cAMP on the DNA-binding domain. Despite changes in the conformation and structural dynamics, cAMP binding does not alter significantly the secondary structural composition of the wild-type CRP. The apparent difference between functional and nonfunctional analogues of cAMP is the ability of cAMP to effect an increase in the dynamic motions of the DNA binding domain.

Cyclic AMP receptor protein (CRP)[1] plays a key role in the regulation of expression of a large number of genes in *Escherichia coli* (*1*, *2*). CRP exists as a dimeric protein composed of two chemically identical subunits with 209 amino acid residues and two cAMP binding sites per subunit (*3*). The functional activities of CRP as a transcription regulatory factor are controlled by the cellular concentration of cAMP. In the presence of cAMP, CRP undergoes a conformational change leading to the recognition of specific DNA sequence and interaction with RNA polymerase (*1*, *4*). X-ray crystal structures of cAMP-liganded CRP revealed that each subunit contains two domains: a larger amino terminal domain (residues 1−133), which contains the cAMP-binding site, and a smaller carboxyl terminal domain (residues 139−209), which binds to DNA through a helix−turn−helix motif (*5*−*7*). The two functional domains are connected covalently by a stretch of polypeptides denoted as the hinge region (residues 134−138), which runs between the C α-helix of the cAMP-binding domain and the D α-helix of the DNA-binding domain. A bias of distribution in secondary structure is found between the two functional domains. The larger cAMP-binding domain contains predominantly β-sheet structure, whereas the smaller DNA-binding domain is composed principally of α-helices (*5*, *7*), as shown in Figure 1.

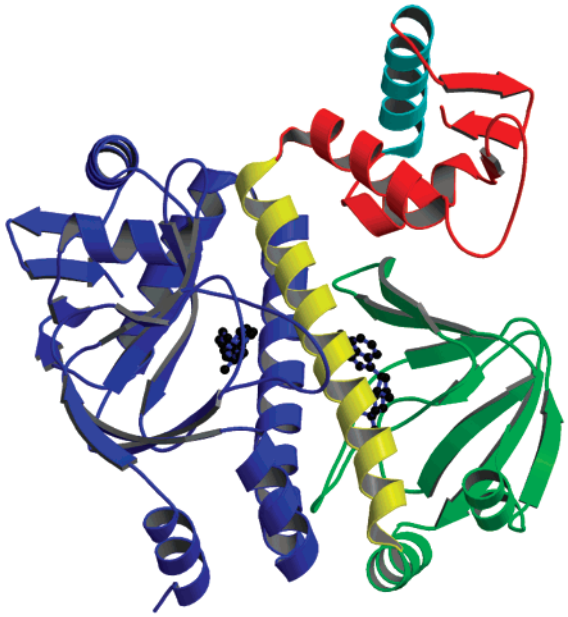

FIGURE 1: Structure of CRP dimer. In one subunit, the green and red domains indicate the cAMP and DNA binding domains, respectively. The C helix, which is involved in intersubunit interaction, is in yellow. The DNA recognition F helix is in cyan. cAMP is shown in black. The other subunit is in blue. Structure was generated using coordinates of CRP (1G6N) from the RCSB Protein Data Bank (http://www.rcsb.mg/pbd/).

† Supported by NIH Grant GM-45579 and by Grants H-0013 and H-1238 from the Robert A. Welch Foundation. J.M. was partially supported by a Fulbright Fellowship, Institute of International Education, NY.

* To whom correspondence should be addressed. Phone: (409) 772-2281. Fax: (409) 772-4298. E-mail: jclee@utmb.edu.

‡ University of Texas Medical Branch.

§ On sabbatical leave from the University of Northern Colorado.

|| University of Colorado Health Sciences Center.

[1] Abbreviations: CRP, cyclic AMP receptor protein; cAMP, cyclic AMP; cGMP, cyclic GMP; H−D exchange, hydrogen−deuterium exchange; FT-IR, Fourier transform infrared.

10.1021/bi020036z CCC: $22.00
Published on Web 05/04/2002

There is mounting evidence to suggest that CRP undergoes allosteric conformational changes upon cAMP binding from a variety of spectroscopic and biochemical techniques including small-angle X-ray scattering (*8*), small angle neutron scattering (*9*), NMR (*10*,*11*), Raman (*12*), proteolytic digestion (*13*−*16*), protein footprinting (*17*), isothermal titration calorimetry (*18*), and fluorescence (*19*, *20*). Although the exact nature of this conformational change remains elusive because of the lack of high-resolution structural information of apo-CRP, it has been postulated that the cAMP-induced conformational changes are likely to include reorientation of subunits with respect to each other and reorientation of DNA-binding domain relative to cAMP-binding domain within the same subunit (*5*, *21*). The proposed cAMP-induced conformational changes represent rigid-body movements of structural elements without significant changes in secondary structures. Results of a comparative study of the NMR structure of apo-CRP in solution and known crystal structure of cAMP-liganded CRP lend support to the proposed change (*11*).

Wild-type CRP is activated by cAMP only, although it can bind other cyclic nucleotides with comparable affinity (*22*). Most often, as in this study, cGMP is employed as a nonfunctional analogue of cAMP to investigate the differential effects of these ligands.

As a result of investigating eight CRP mutants, a recent study concluded that the CRP molecule is designed with a high degree of plasticity. CRP most likely exists as an ensemble of dynamic states. Binding of ligands and mutations exert their effects by altering the distribution of these dynamic states (*23*). However, several important questions remain unanswered. Are there structural dynamics changes associated with the cAMP-induced conformational changes? How important are the structural dynamics changes to CRP biological function? To address these questions, the cyclic nucleotide-induced changes in the conformation and structural dynamics of wild-type CRP were investigated by hydrogen−deuterium (H−D) exchange and Fourier transform infrared (FT-IR) spectroscopy. When the spectral change as a result of H−D exchange at the amide I regions associated with specific secondary structural elements is monitored, these data indicate that upon the binding of cAMP the two functional domains of CRP undergo structural dynamics changes in opposite directions. While the smaller DNA-binding domain becomes more flexible, the larger cAMP-binding domain shifts to a more rigid or more compact conformation.

MATERIALS AND METHODS

Materials. Wild-type CRP was isolated and purified from *E. coli* as described previously (*15*) and then stored in a −20 °C freezer until use. Cyclic AMP and cyclic GMP were purchased from Sigma (St. Louis, MO). Deuterium oxide (99.96 atom % D) was the product of Cambridge Isotope Laboratories (Andover, MA). The stock solutions of cAMP (18.4 mM) and cGMP (23.5 mM) were prepared by dissolving cyclic nucleotides in 50 mM Tris, 0.1 M KCl, and 1 mM EDTA (pH 7.8), and the pH was adjusted with KOH solution. The concentrations of cAMP and cGMP were determined spectrophotometrically using the extinction coefficients of 14 650 M^{-1} cm^{-1} at 258 nm for cAMP and 12 950 M^{-1} cm^{-1} at 254 nm for cGMP (The Merck Index).

Protein Preparations. CRP solution was dialyzed against 50 mM Tris buffer containing 0.1 M KCl and 1 mM EDTA, pH 7.8, overnight to remove the stabilizing agent glycerol and other additives. The resultant was concentrated with a Centricon 10 microconcentrator (Amicon) at 5000 rpm using an SS-34 rotor. The concentration of the stock CRP solution was determined spectrophotometrically using the extinction coefficient of 40 800 M^{-1} cm^{-1} at 278 nm for the CRP dimer (*22*). The cAMP- or cGMP-liganded CRP samples were prepared by adding aliquots of a stock solution of cAMP or cGMP to CRP solutions in a molar ratio of 5:1 prior to H−D exchange or FT-IR measurement. This ratio was used to ensure cyclic nucleotide saturation of the high-affinity binding sites according to their binding constants[2] (*15*). Although there is another set of cAMP binding sites, their affinity is about 100-fold weaker. Thus, in this study the effects of ligands mostly reflect that of the binding to the high affinity sites, the occupancy of which elicit activation of CRP. The H−D exchange was carried out by mixing aliquots of stock solution of CRP, after adjusting buffer concentration, with D_2O at a percentage ratio of 50:50 or 20:80 H_2O/D_2O prior to FT-IR measurement.

FT-IR Spectroscopy. FT-IR spectra were measured with a Bomem MB series FT-IR spectrometer (Quebec, Canada) equipped with a dTGS detector and purged constantly with dry air generated by a Balston (Haverhill, MA) air dryer. Protein samples (12 mg/mL for H_2O and 3.0 mg/mL for H_2O/D_2O) were loaded in a part number 20500 heatable liquid IR cell (Graseby) with CaF_2 windows and a 6 μm spacer for H_2O solution and a 25 μm spacer for H_2O/D_2O solutions. For each spectrum, a 128-scan interferogram was collected in single-beam mode with a 4 cm^{-1} resolution. The scan accumulation time was 6 $^1/_2$ minutes. Reference spectra were recorded under identical scan conditions with only the corresponding buffer in the cell. For the H−D exchange experiment, the time points refer to the scan starting times. Protein spectra were obtained according to previously established criteria and a subtraction procedure (*24*). The residual water vapor signals, if present, in the spectrum of protein were removed by subtracting the spectrum of gaseous water. Second-derivative spectra were obtained with a seven-point Savitsky−Golay derivative function. All second-derivative spectra were baseline-corrected and area-normalized as previously described (*25*). Final spectra were treated with a 2*X* interpolate function and plotted with a SigmaPlot 5 software (Jandel Scientific). Secondary structure content of the apo-CRP was determined by curve-fitting analysis of the inverted second-derivative spectrum as described previously (*26*).

RESULTS

FT-IR Spectra of CRP in H_2O Solution. Figure 2 shows the second-derivative amide I spectra of CRP in 50 mM Tris buffer, pH 7.8, containing 0.1 M KCl and 1 mM EDTA. The spectra of apo and cAMP- and cGMP-liganded species are superimposed to facilitate comparison. All spectra exhibited four basic band components that can be assigned to the α-helix (∼1656 cm^{-1}), β-sheet (∼1635 cm^{-1}), and β-turns (1685 and 1675 cm^{-1}) on the bases of previous

[2] S.-H. Lin and J. C. Lee, manuscript to be submitted.

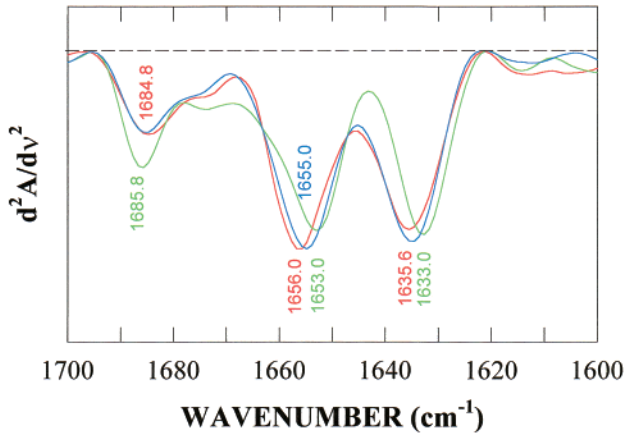

FIGURE 2: Second-derivative amide I spectra of apo, cAMP-liganded, and cGMP-liganded CRP in H_2O solution. The solution composition and color of the line are the following: (red), apo-CRP; (green), cAMP−CRP complex; (purple), cGMP−CRP complex.

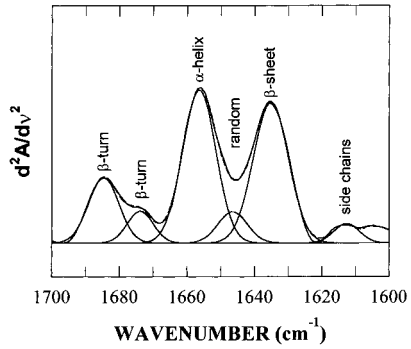

FIGURE 3: Curve-fitted inverted second-derivative amide I spectrum of apo-CRP. The inversion of second-derivative spectrum was done by factoring by −1. The curve-fitting was carried out as described under Materials and Methods.

infrared studies of other proteins in aqueous solution (*24*). An additional band component at 1647 cm^{-1}, ascribable to random structure, was revealed by the curve-fitting procedure (Figure 3). Quantitative analysis by curve-fitting shows that the apo-CRP contains 37% α-helix, 36% *β*-sheets, 20% *β*-turns, and 7% random structures. Although no high-resolution structural information is currently available for the apo-CRP, this result agrees closely with the values of 36.4% α-helix and 35.4% *β*-sheet for cAMP-liganded CRP obtained by X-ray crystallography (*5*) and is generally consistent with the values reported by Raman spectroscopy for the apo-CRP (44% α-helix, 28% *β*-sheet, 18% turn, and 10% undefined) (*12*).

Binding of ligands shifts the α-helix and *β*-sheet bands to lower wavenumbers. Binding of cAMP induces a 3 cm^{-1} downshift in the α-helix band and a 2.6 cm^{-1} downshift in the *β*-sheet band, whereas binding of cGMP induces about a 1 cm^{-1} downshift in the α-helix and *β*-sheet bands. The ligand-induced changes in peak wavenumber of the α-helix and *β*-sheet bands indicate conformational changes at tertiary and quaternary structural levels, leading to an environmental alteration for the α-helix and *β*-sheet structures. The ligand-induced change in the α-helix band frequency likely originated from changes in two regions, namely, the DNA-binding domain (D, E, and F α-helices) and the subunit interface (C α-helices). Any possible change at the A and B α-helices is not expected to affect the frequency of the α-helix band because of their surface locations and the relatively small number of residues that constitute these helices (*5*, *7*). Since the vibrational energy of the amide C═O stretching is inversely related to the strength of hydrogen bonding, the downshift in the α-helix and *β*-sheet band wavenumbers induced by binding cAMP implies a strengthening in hydrogen bonding within α-helix and between *β*-strands (*27*).

No emphasis has been placed on the intensity difference at individual bands between the spectra of apo and cyclic nucleotide-liganded forms. These measurements in H_2O are difficult because of potential distortional effects of cyclic nucleotide-induced perturbation at high protein concentration (∼12 mg/mL) required for obtaining high-quality spectra in H_2O-based solution. Various degrees of perturbation were observed when cyclic nucleotide was added to the protein solutions.

FT-IR Spectra of CRP in the 50:50 and 20:80 H_2O/D_2O H−D Exchange. To identify the origin of ligand-induced changes in α-helix band frequencies and to explore any related change in structural dynamics of CRP, H−D exchange experiments were conducted in two solutions of different percentage ratios of H_2O/D_2O, namely, 50:50 and 20:80. The basic considerations for this experiment are as follows: (1) by variation of the availability of deuterium in bulk solution, a selected level of structural dynamics of the proteins can be detected; (2) by reduction of the availability of deuterium in bulk solution relative to that in 100% D_2O, the fast amide proton exchange can be singled-out for analysis.

Figure 4 shows the second-derivative amide I spectra of CRP in the absence and presence of cAMP or cGMP in a percentage ratio of 50:50 H_2O/D_2O solution as a function of time. The spectrum of apo-CRP in H_2O solution is included for reference. Shifts to lower wavenumber and decrease in band intensity are signatures of H−D exchange (*28*). As shown in Figure 4, in all cases immediately after mixing of the protein solution with D_2O, significant intensity reduction was observed at the band assigned to *β*-turns (∼1685 cm^{-1}). This result indicates a rapid H−D exchange in these *β*-turns. In turn, it reflects the fact that the *β*-turn structures are generally located at the surface of proteins with high degree of solvent exposure. The most remarkable changes, however, were observed at the bands assigned to the α-helix and *β*-sheet structures. Immediately after mixing of the protein solution with D_2O, both the α-helix and *β*-sheet bands shifted to lower wavenumbers, accompanied by intensity changes that vary among CRP species. These observations indicate a H−D exchange and that the pattern of exchange is dependent on the specific ligand present.

In addition to a shift to 1634 cm^{-1}, a marked intensity decrease at the *β*-sheet band was observed for apo-CRP as a function of time, accompanied by an intensity increase near 1640 cm^{-1}, as shown in Figure 4A. The result implies that a significant portion of *β*-sheet structures in apo-CRP is fairly flexible, which allows an observable amide proton exchange to occur during the course of experiment. The H−D-exchange-induced *β*-sheet band splitting and shift to higher wavenumber during the course of H−D exchange are not uncommon and have been reported earlier for *β*-lactoglobulins (*31*). In addition, significant intensity reduction near 1653 cm^{-1} (combination of unexchanged and exchanged

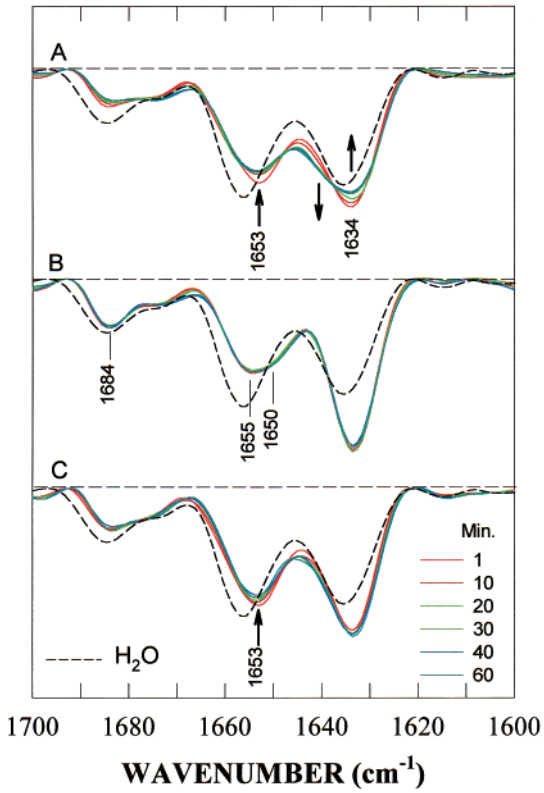

FIGURE 4: Second-derivative amide I spectra of CRP in a percentage ratio of 50:50 H_2O/D_2O solution as a function of time: (A) spectra of apo-CRP; (B) spectra of cAMP−CRP complex; (C) spectra of cGMP−CRP complex. The spectra were recorded at 1, 10, 20, 30, 40, and 60 min (starting times) after the sample mixing. The arrows indicate the directions in which the intensities of the bands are shifting with time. The spectrum of apo-CRP in H_2O (- - -) is included for reference.

α-helices) as a function of time was also observed. The overall intensity decrease at the α-helix band might be interpreted to reflect the amount of amide protons exchanged.

For the cAMP−CRP complex, H−D exchange resulted in two populations of α-helices, represented by the bands near 1655 and 1650 cm^{-1}, as shown in Figure 4B. The former represents the α-helices with unexchanged amide hydrogen, and the latter represents the α-helices with exchanged amide deuterium (*28*−*30*). The likely candidates for the H−D exchanged α-helices are the A, B, and F α-helices. The likely candidates for the unexchanged α-helices are the C, D, and E α-helices. The overall intensity at the *β*-sheet region was significantly increased as a result of exchange-induced intensity redistribution of non-*β*-sheet structure (i.e., *β*-turn and random structures) in combination with a relatively slow amide proton exchange of the *β*-sheet structure (*28*, *31*). Almost no time-dependent intensity change at both the α-helix and *β*-sheet regions was observed beyond the initial exchange in cAMP-liganded CRP. Since the DNA-binding domain is primarily α-helices (*5*), the observation of the appearance of the shoulder at 1650 cm^{-1} at the first time point indicates that in the DNA-binding domain some helices are highly dynamic in the presence of cAMP. Because the intensity should decrease with H−D exchange, the lack of change of intensity with time at 1650 and 1655 cm^{-1} implies fast exchange in some helices but not in others under these experimental conditions. These results imply that the exchange was so rapid that it was completed by the first time point and no H−D exchange occurred within the time frame of this study. The intensity of the 1634 cm^{-1} band was significantly greater than that of apo-CRP (Figure 4A). This implies that a greater number of amide protons in the *β*-sheets are not exchanging. Since the cAMP-binding site is largely composed of *β*-sheets, this result indicates that the binding of cAMP reduces the structural dynamics of the cAMP-binding domain.

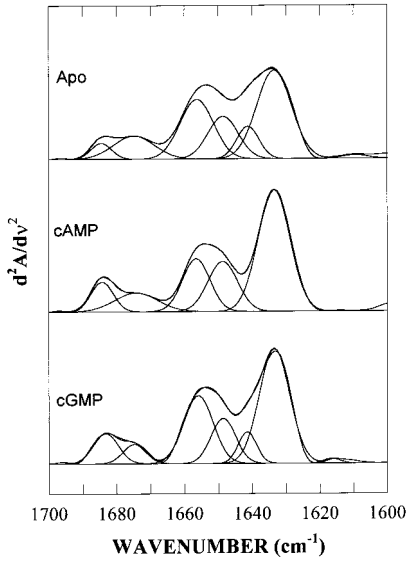

FIGURE 5: Curve-fitted inverted second-derivative amide I spectra of apo, cAMP-liganded, and cGMP-liganded CRP. The spectra recorded at 60 min after H−D exchange were selected from Figure 4.

For the cGMP-liganded CRP, somewhat different H−D exchange behavior was observed in both the α-helix and *β*-sheet regions, as shown in Figure 4C. Its *β*-sheet band near 1634 cm^{-1} was less intense than that of the cAMP-liganded counterpart but more intense than that of the apo form. Its α-helix band at 1653 cm^{-1} is the most intense one among all three species. This H−D exchange behavior indicates that the binding of cGMP stabilizes the cAMP-binding domain, but it fails to relax the α-helices of DNA binding domain. The result implies that the effects of cGMP on the structural dynamics of CPR differ significantly from the effects of cAMP.

To test if the ligand-induced spectral changes are consistent among the three species, a detailed spectral analysis was conducted using curve-fitting on a set of selected spectra. Figure 5 shows the curve-fitted inverse second-derivative spectra that were measured after 60 min of H−D exchange in 50:50 H_2O/D_2O solution. Detailed parameters are presented in Table 1. There is almost no time-dependent change for the cAMP-liganded CRP within 60 min of H−D exchange. Nearly $^2/_3$ of α-helix structures in apo and cGMP-liganded forms remained unexchanged, whereas one-half of α-helix structures in cAMP-liganded form changed their amide hydrogen to deuterium at the beginning of the experiment. Thus, the area analyses of the data showed that cAMP binding induced rapid exchange in the α-helices in contrast to apo and the cGMP−CRP complex. Despite a higher intensity of its 1634 cm^{-1} band, cAMP-liganded CRP has a similar *β*-sheet band area (47%) as its apo (44%) and cGMP-liganded (49%) counterparts.

Table 1: Frequencies and Relative Areas of Amide I Components of CRP after 60 min of H−D Exchange in 50:50 H_2O/D_2O Solutions

apo		cAMP-liganded[a]		cGMP-liganded		
ν (cm^{-1})	area (%)	ν (cm^{-1})	area (%)	ν (cm^{-1})	area (%)	assignment
1684.5	3.8	1684.3	8.0	1683.2	8.9	β-turn
1674.9	13.6	1674.3	9.7	1674.8	5.4	β-turn
1656.3	23.2	1656.6	17.6	1656.2	24.0	α-helix (H)[b]
1648.6	15.1	1648.7	17.9	1648.6	13.3	α-helix (D)[c]
1641.2	8.4		0	1641.5	6.7	β-sheet
1633.5	35.9	1633.5	46.8	1633.5	41.7	β-sheet

[a] The time-dependent changes for cAMP-liganded CRP between the spectra measured at 1 and 60 min were very small. [b] α-Helices with unexchanged amide hydrogen. [c] α-Helices with exchanged amide deuterium.

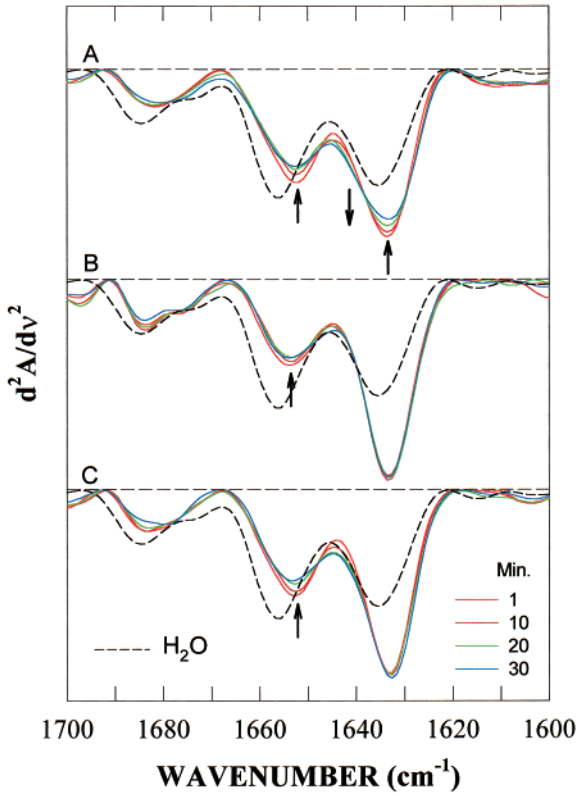

FIGURE 6: Second-derivative amide I spectra of CRP in a percentage ratio of 20:80 H_2O/D_2O solution as a function of time: (A) spectra of apo-CRP; (B) spectra of cAMP−CRP complex; (C) spectra of cGMP−CRP complex. The spectra were recorded at 1, 10, 20, and 30 min (starting times) after the sample mixing. The arrows indicate the directions in which the intensities of the bands are shifting with time. The spectrum of apo-CRP in H_2O (- - -) is included for reference.

Figure 6 shows the second-derivative amide I spectra of wild-type CRP in the absence and presence of cAMP or cGMP in a percentage ratio of 20:80 H_2O/D_2O solution as a function of time. By increasing the availability of deuterium in bulk solution, one can potentially expand the probe into the structural dynamics of much less accessible regions of the proteins. By comparison with the protein in 50:50 H_2O/D_2O solution, further exchange-induced changes in intensity were observed in the bands assigned to the α-helix structure in all three species. Unlike its apo and cGMP-liganded counterparts, cAMP−CRP exhibited a smaller band near 1653 cm^{-1} (combination of exchanged and unexchanged α-helices), indicating further amide proton exchange in the

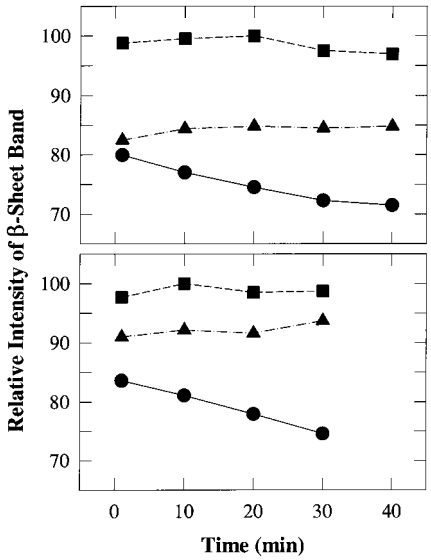

FIGURE 7: Effects of cyclic nucleotides on the structural dynamics of β-sheet structures of CRP as revealed by time-dependent changes in the relative intensity of β-sheet bands at 1634 cm^{-1} in 50:50 (upper panel) and 20:80 (lower panel) H_2O/D_2O solutions: apo (●), cAMP-liganded (■), and cGMP-liganded (▲) species. The values of relative intensities were normalized using the highest intensity value in each H_2O/D_2O ratio group as 100%.

α-helix structure, as shown in Figure 6B. After an initial intensity increase due to redistribution of H−D exchanged structural elements, a reduction in the β-sheet band intensity was observed for the apo-CRP as a function of time, as shown in Figure 6A, but not for cAMP- and cGMP-liganded forms.

Figure 7 shows the plots of the relative intensity change at the 1634 cm^{-1} β-sheet band of CRP in 50:50 (upper panel) and 20:80 (lower panel) H_2O/D_2O solution as a function of time. The intensity of the β-sheet band was calculated as a difference in the second-derivative spectrum between the negative peak at maximum and the baseline. The values of relative intensities were normalized using the highest intensity value in each H_2O/D_2O ratio group as 100%. It is pointed out that under these conditions of partial H−D exchange, the intensity value at a given frequency is determined not only by the content of a specific secondary structural element but also by changes in band shape and other factors such as redistribution of the components with exchanged amide deuterium. Although the relative intensity changes may be an approximation, the approximation avoids the much greater ambiguity associated with the alternative curve-fitting approach due to uncertainty in multiple-component involvement. In this case, the subsequent change in relative intensity of the β-sheet band does reflect the extent of amide proton exchange in the β-sheet structure of the protein, as shown in Figure 5 and Table 1. For a given CRP species, the β-sheet band with higher relative intensity means lesser amide proton exchange, which in turn suggests a lesser structural dynamics involving the cAMP-binding domain.

DISCUSSION

Conformation and structural dynamics are essential to proteins for carrying out proper biological functions. Ligand-induced allosteric conformational change is among the most recognized phenomena in protein structural biology and has

been known to play important roles in the functions of countless proteins. The structural dynamics of a given conformation is likely to influence the activity of the protein. In the past few decades, H−D exchange has been used extensively in studies of the structural dynamics of proteins (*32*−*34*). It has been established that the rates at which the amide proton exchanges with solvent deuterium reflect the structural dynamics of proteins (*35*) and they are sensitive to secondary structural composition and experimental conditions such as pH, temperature, and pressure (*32*−*34*). At constant experimental conditions, a more rapid rate of exchange implies a greater flexibility and motion in the structural region of the exchange. The exchangeable amide protons that are involved in hydrogen-bonded structures can exchange with solvent deuterium only when they are transiently exposed to the solvent catalyst. In addition, the hydrogen-bond donor−acceptor pair has to be separated by 5 Å or more (*34*).

Despite extensive use of D_2O solvent in FT-IR spectroscopic studies of proteins, few investigators have taken advantage of partial H−D exchange to study the structural dynamics of proteins at more basic structural levels. Most of infrared structural dynamics studies were focused on H−D exchange of proteins on a global scale (*32*−*34*, *36*, *37*). In the present study, the usefulness of the partial H−D exchange was explored to probe the ligand-induced structural dynamics changes of the protein at more specific structural regions. The results demonstrate that by limitation of the availability of deuterium in the bulk solution, the ligand-induced structural dynamics changes at the secondary structure and subdomain levels can be detected and analyzed. The bias in the distribution of secondary structural elements between the two functional domains of CRP, namely, extensive β-sheet structure in cAMP-binding domain and predominant α-helix structure in DNA-binding domain (*5*, *7*), facilitates the interpretation of the cyclic-nucleotide-induced conformational and structural dynamics changes of CRP.

Cyclic-Nucleotides-Induced Change at the α*-Helix Band in H_2O Solution*. There are two sets of cAMP binding sites, namely, high- and low-affinity sites. Occupancy of the high-affinity sites activates CRP for the specific DNA binding, while the occupancy of the low-affinity site(s) elicits lower affinity for DNA. In this study, the effects of cAMP on CRP as an activator are probed; thus, the concentration of cAMP was carefully chosen to maximize the effects of cAMP binding to the high-affinity sites while minimizing that to the weak site. The cAMP-induced large change in wavenumber at the α-helix band likely resulted from relaxation of the environment surrounding the α-helices. A parallel example of the downshifted α-helix band due to a more relaxed environment can be found between two heme proteins: myoglobin and hemoglobin. With nearly identical secondary structure arrangement, the α-helix band of monomeric myoglobin (1654 cm^{-1}) is 2 cm^{-1} lower than that of tetrameric hemoglobin (1656 cm^{-1}) (*38*). For a fully solvated α-helix without the protection of the tertiary fold of protein, a much lower wavenumber (between 1645 and 1630 cm^{-1}) may be expected (*30*, *39*).

The cAMP-mediated allosteric conformational changes in CRP involving α-helix structures in two structural regions, the DNA-binding domain (D, E, and F helices) and the subunit interface (C α-helices), have long been proposed (*5*, *19*). Most recently, by mapping the functionally important residues on the refined cAMP−CRP structure, Passner and colleagues (*7*) speculated that a cAMP-induced allosteric transition might involve a change in the orientation of the DNA-binding domain relative to cAMP-binding domain. This change is presumably preceded by a reorientation of C α-helices with respect to each other at the subunit interface.

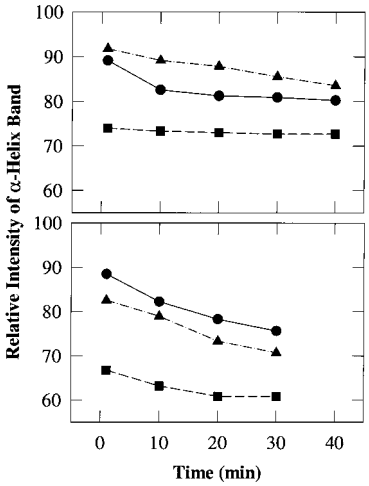

FIGURE 8: Effects of cyclic nucleotides on relative intensity of the α-helix band of CRP in 50:50 (upper panel) and 20:80 (lower panel) H_2O/D_2O solutions as functions of time: apo (●), cAMP-liganded (■), and cGMP-liganded (▲) species. The values of relative intensities were normalized using the value of apo-CRP in H_2O as 100%.

The cAMP-induced conformational changes at either the subunit interface or the DNA-binding domain could result in a change in the wavenumber in the α-helix band. Among the three species, namely, apo-CRP, cAMP−CRP, and cGMP−CRP complexes, the cAMP-liganded CRP displayed the lowest wavenumber for the α-helix band (Figure 2); i.e., cAMP binding induced the most significant change in the environment of the helices. Additional information gleaned from the partial H−D exchange experiments will assist in the identification of the cAMP-induced frequency change at the α-helix band in H_2O solution. Figure 8 shows the plots depicting the relative intensity changes at the bands assigned to the α-helix structure of CRP. The intensity of the α-helix band was calculated as the difference between the negative peak at maximum (1656−1653 cm^{-1}) and the baseline in the second-derivative spectra. The values of the relative intensities were normalized for all three species using the value of 100% for apo-CRP measured in H_2O solution. Regardless of the ratio of H_2O/D_2O, as shown in the upper and lower panels of Figure 8, even at the first time point, significant differences in the relative intensity of α-helix bands were observed between the cAMP-liganded and apo forms. In the cAMP−CRP complex, only 65−75% intensity was observed compared to the ∼90% in apo-CRP. These results indicate a cAMP-induced acceleration in the amide proton exchange of the α-helix structure. However, cGMP induced a different phenomenon. In 50:50 H_2O/D_2O (Figure 8, upper panel) in the cGMP−CRP complex a higher percentage of intensity compared with that for apo-CRP was observed at each time point. These results suggest that binding of cGMP retarded a small amount of the amide proton exchange of the α-helices. However, when deuterium becomes more readily available for exchange as in 20:80

H_2O/D_2O (lower panel), the remaining amide protons exchange with a rate similar to that in apo and in the cAMP−CRP complex.

There is an apparent relationship between the downshift in wavenumber of the α-helix band in H_2O and the extent of H−D exchange of the α-helix structure in D_2O. It may be concluded that the ligand-induced conformational change at the subunit interface (C α-helices) and the DNA-binding domain most likely account for the downshift in wavenumber at the α-helix band in H_2O solution and for differences in the extent of amide I proton exchange at the α-helices. These results are consistent with the interpretation that cAMP induces a significant increase in the dynamics in helices while cGMP induces less. It is noteworthy that the ligand-induced change in either the α-helix or *β*-sheet bands, observed in H_2O solution, has not been observed for CRP in H_2O/D_2O solution (Table 1).

Upon binding of cAMP, the wild-type CRP undergoes intrasubunit, as well as intersubunit, conformational changes. The intrasubunit conformational changes involving its two functional domains proceed in opposite directions. While the conformation of the smaller DNA-binding domain changes to a more flexible structure, the larger cAMP-binding domain shifts to a more rigid or compact structure. The cAMP-induced changes involve the α-helix structures in both the subunit interface and the DNA-binding domain. This result is consistent with the results from NMR (*10*) and small-angle neutron scattering measurements (*9*). It is also consistent with the result from NMR (*11*) and protein footprinting (*17*) that the F α-helix becomes more exposed to the surface of the protein as a result of cAMP binding.

No comparable relaxation effect on the DNA-binding domain was observed for cGMP-liganded CRP relative to its cAMP-liganded counterpart. Instead, a significant retardation in the amide proton exchange of the α-helix structure was observed. To a lesser extent, cGMP binding appears to be able to produce structural dynamics changes at the cyclic-nucleotide-binding domain similar to that induced by cAMP.

During H−D exchange, the intensity of the *β*-sheet band becomes stronger. The increase in the *β*-sheet band area of CRP (i.e., 44% in D_2O vs 36% in H_2O for apo-CRP) was confirmed by the curve-fitting analysis (Table 1). This apparent increase in area should not be automatically ascribed to a change in the secondary structural composition. An equally likely scenario is that some of the band intensities assigned to the *β*-turn and random structures in H_2O have redistributed into the regions assigned to the *β*-sheet structures in D_2O. This result implies that caution must be exercised when calculating the secondary structure composition of a protein based solely on the infrared spectrum obtained in D_2O solvent.

CONCLUSIONS

Binding of cAMP to wild-type CRP induces conformational and structural dynamics changes in opposite directions in the cAMP-binding domain and DNA-binding domain. While the cAMP-binding domain was tightened up and the structural dynamics of *β*-sheet structures was constrained, cAMP-binding relaxes the α-helix structure in the DNA-binding domain, presumably enabling it to interact easily with the DNA molecule. To a lesser extent, binding of cGMP produces similar tightening effects on the cyclic-nucleotide-binding domain as cAMP, but it fails to mimic the relaxation effect of cAMP on the DNA-binding domain. This study reveals a novel mode of activation of CRP by cAMP. The cAMP-induced increase in structural dynamics in the DNA binding domain could conceivably provide the DNA-recognizing F helices with the plasticity to fit into the DNA grooves. This might be the mechanism employed by CRP to bind to so many different DNA promoter sequences, since CRP is known to be involved in the regulation of the transcription of more than 20 genes (*1*, *40*). Each promoter sequence is different except for the two half-sites with the consensus sequence TGTGA...XCAXA. An increase in the dynamics of the helices would enable the DNA-recognizing helices to fit into a variety of DNA base sequences. The challenge is in acquiring specific information on the identity of the helices whose dynamics properties have been altered by cAMP binding, since FT-IR only identifies the class of secondary structure.

ACKNOWLEDGMENT

The authors appreciate critical review of the manuscript by members of the Lee lab, especially S.-H. Lin and E. Czerwinski for Figure 1.

REFERENCES

1. Kolb, A., Busby, S., Bus, H., Garges, S., and Adhya, S. (1993) *Annu. Rev. Biochem. 62*, 749−795.
2. Harman, J. G. (2001) *Biochim. Biophys. Acta 1547*, 1−17.
3. Passner, J. M., and Steitz, T. A. (1997) *Proc. Natl. Acad. Sci. U.S.A. 94*, 2843−2847.
4. Botsford, J. L., and Harman, J. G. (1992) *Microbiol. Rev. 56*, 100−122.
5. Weber, I. T., and Steitz, T. A. (1987) *J. Mol. Biol. 198*, 311−326.
6. Schultz, S. C., Shields, G. C., and Steitz, T. A. (1991) *Science 253*, 1001−1007.
7. Passner, J. M., Schultz, S. C., and Steitz, T. A. (2000) *J. Mol. Biol. 304*, 847−859.
8. Kumar, S. A., Murthy, N. S., and Krakow, J. S. (1980) *FEBS Lett. 109*, 121−124.
9. Krueger, S., Gorshkova, I., Brown, J., Hoskins, J., McKenney, K. H., and Schwarz, F. P. (1998) *J. Biol. Chem. 273*, 20001−20006.
10. Gronenborn, A. M., and Clore, G. M. (1982) *Biochemistry 21*, 4040−4047.
11. Won, H.-S., Yamazaki, T., Lee, T.-W., Yoon, M.-K., Park, S.-H., Kyogoku, Y., and Lee, B.-J. (2000) *Biochemistry 39*, 13953−13962.
12. DeGrazia, H., Harman, J., Tan, G.-S., and Wartell, R. M. (1990) *Biochemistry 29*, 3557−3562.
13. Eilen, E., Pampeno, C., and Krakow, J. S. (1994) *Biochemistry 17*, 2469−2473.
14. Krakow, J. S., and Pastan, I. (1973) *Proc. Natl. Acad. Sci. U.S.A. 70*, 2529−2533.
15. Heyduk, T., and Lee, J. C. (1989) *Biochemistry 28*, 6914−6924.
16. Cheng, X. D., Kovac, L., and Lee, J. C. (1995) *Biochemistry 34*, 10816−10826.
17. Baichoo, N., and Heyduk, T. (1997) *Biochemistry 36*, 10830−10836.
18. Gorshkova, I., Moore, J. L., McKenney, K. H., and Schwarz, F. P. (1995) *J. Biol. Chem. 270*, 21679−21683.
19. Wu, C.-W., and Wu, F. Y.-H. (1974) *Biochemistry 13*, 2573−2578.
20. Malecki, J., Polit, A., and Wasylewski, Z. (2000) *J. Biol. Chem. 273*, 8480−8486.
21. Garges, S., and Adhya, S. (1985) *Cell 41*, 745−751.
22. Cheng, X., and Lee, J. C. (1994) *J. Biol. Chem. 269*, 30781−30784.

23. Lin, S.-H., Kovac, L., Chin, A. J., Chin, C. C. Q., and Lee, J. C. (2002) *Biochemistry 41*, 2946−2955.
24. Dong, A., and Caughey, W. S. (1994) *Methods Enzymol. 232*, 139−175.
25. Dong, A., Prestrelski, S. J., and Carpenter, J. C. (1995) *J. Pharm. Sci. 84*, 415−424.
26. Dong, A., Caughey, B., Caughey, W. S., Bhat, K. S., and Coe, J. E. (1992) *Biochemistry 31*, 9364−9370.
27. Krimm, S., and Bandekar, J. (1986) *Adv Protein Chem. 38*, 181−364.
28. Susi, H., and Byler, D. H. (1986) *Methods Enzymol. 130*, 290−311.
29. Williams, S., Causgrove, T. P., Gilmanshin, R., Fang, K. S., Callender, R. H., Woodruff, W. H., and Dyer, R. B. (1996) *Biochemistry 35*, 691−697.
30. Gilmanshin, R., Williams, S., Callender, R. H., Woodruff, W. H., and Dyer, R. B. (1997) *Proc. Natl. Acad. Sci. U.S.A. 94*, 3709−3713.
31. Dong, A., Matssura, J., Allison, S. D., Chrisman, E., Manning, M. C., and Carpenter, J. F. (1996) *Biochemistry 35*, 1450−1457.
32. Hvidt, A., and Nielsen, S. O. (1966) *Adv. Protein Chem. 21*, 287−386.
33. Woodward, C. K., and Hilton, B. D. (1979) *Annu. Rev. Biophys. Bioeng. 8*, 99−127.
34. Englander, S. W., and Kallenbach, N. R. (1983) *Q. Rev. Biophys. 16*, 521−655.
35. Englander, S. W. (2000) *Annu. Rev. Biophys. Biomol. Struct. 29*, 213−238.
36. Milne, J. S., Mayne, L., Roder, H., Wand, A. J., and Englander, S. W. (1998) *Protein Sci. 7*, 739−745.
37. Baenziger, J. E., and Methot, N. (1995) *J. Biol. Chem. 270*, 29129−29137.
38. Dong, A., Huang, P., Caughey, B., and Caughey, W. S. (1995) *Arch. Biochem. Biophys. 316*, 893−898.
39. Reisdorf, W. C., Jr., and Krimm, S. (1996) *Biochemistry 35*, 1383−1386.
40. de Crombrugghe, B., Busby, S., and Buc, H. (1984) *Science 244*, 831−838.

BI020036Z